The fully coupled effects of FPSO with different filling ratio tanks in CFD method

Yuan Zhuang*, Decheng Wan‡

State Key Laboratory of Ocean Engineering, School of Naval Architecture, Ocean and Civil Engineering, Shanghai Jiao Tong University, Collaborative Innovation Center for Advanced Ship and Deep-Sea Exploration, Shanghai 200240, China

*Presenting author: nana2_0@sjtu.edu.cn

‡Corresponding author: dcwan@sjtu.edu.cn

http://dcwan.sjtu.edu.cn

Abstract

With the increasing demand of oil and natural gas, the FPSO with LNG tanks was proposed as a popular type LNG platform. Equipped with liquid natural gas so that the tanks has free surface during the operation, FPSO will suffer from sloshing forces and moments from inner tanks. At the meantime, the sloshing flow in tanks is influenced by the ship motion in return. This paper applied numerical methods to study the coupling effects between FPSO and sloshing tanks. The coupling effects were solved in CFD method, using our in house solver naoe-FOAM-SJTU, based on open package toolbox OpenFOAM. The outer field and inner free surface were both simulated by solving Navier-Stocks equation thus the ship motion and sloshing tanks were fully coupled. The two LNG tanks were in different filling conditions, and the sloshing forces and moments were considered in current study.

Keywords: FPSO LNG; sloshing; naoe-FOAM-SJTU solver; fully coupled analysis

Introduction

For the oil and natural gas occupied the main position during the production in recent years, the demand of these energy sources calls for the need of deep sea platform, which has the ability to exploit gas field and process the crude oil in deep water. As a result, FPSO (Floating Production Storage and Offloading) was proposed as a new type of floating LNG (Liquid Natural Gas) platform. With tanks equipped with FPSO, the existence of inner free surface in tanks would alter the motion of FPSO, and the external excitation such as wave force would change the inner free surface in return. Therefore, the coupling effect between ship motion and tank sloshing become an attractive research.

In recent years, many studies have been done on the sloshing tanks coupled with ship motion. Rognebakke and Faltinsen [1] conducted two-dimensional experiments about hull section with two tanks in waves. Later on, they adopted nonlinear theory to simulate the sloshing tanks and the external fluid separately. Newman [2] analyzed ship motion and sloshing tank in a unified approach – he extended panel code WAMIT and defined inner surface as an extension of external fluid surface. Seo et al [3] applied Rankine panel method to solve both ship motion and inner tanks. Since the viscous flow has advantages over linear potential flow in solving violent sloshing, Lee et al [3] developed a potential-viscous hybrid method to solve ship motion with sloshing tanks. Since then, the violent sloshing tanks were solved in CFD methods, such as fluent or OpenFOAM, and the external flow fields were solved in potential theory[4]-[8]. Shen and Wan [9] applied CFD methods both in external fluid and inner fluid to achieve fully coupled analysis. Zhuang and Wan [10] used fully coupled CFD method to simulate FPSO with two LNG tanks in low-filling ratios, and consider the wave breaking and overturning in tanks. Its results showed well agreement with experiments and the ability to simulate the violent flow in tanks.

In this paper, the model scale of FPSO [11] was chosen. The main focus is on the different filling conditions in fore tank and aft tank. The results were compared to the existing experimental results. In order to discuss the function of sloshing fluid in fore and aft tank, the same filling conditions is also considered. The same filling conditions in fore and aft tank is discussed before [10], yet the sloshing forces and moments were not included. This time we added new function into our CFD solver to calculate the sloshing forces and moments, to discover the coupling effects between ship motion and two different filling ratio tanks.

Numerical Methods

Governing Equations

The incompressible Reynolds-Averaged Navier-Stokes equations are adopted in this paper to investigate the viscous flow. Using dynamic deformation mesh, the governing equations are:

$$\nabla \cdot \mathbf{U} = 0 \tag{1}$$

$$\frac{\partial \rho \mathbf{U}}{\partial t} + \nabla \cdot (\rho(\mathbf{U} - \mathbf{U}_g)\mathbf{U}) = -\nabla p_d - \mathbf{g} \cdot \mathbf{x} \nabla \rho + \nabla \cdot (\mu_{eff} \nabla \mathbf{U}) + (\nabla \mathbf{U}) \cdot \nabla \mu_{eff} + f_\sigma + f_s \tag{2}$$

Where $\mathbf{U}$ is velocity field, $\mathbf{U}_g$ is velocity of grid nodes; $p_d = p - \rho \mathbf{g} \cdot \mathbf{x}$ is dynamic pressure; $\mu_{eff} = \rho(\nu + \nu_t)$ is effective dynamic viscosity, in which ν and ν_t are kinematic viscosity and eddy viscosity respectively. ν_t is obtained by k-ω SST turbulence model[12]. f_σ is the surface tension term in two phases model.

The solution of momentum and continuity equations is implemented by using the pressure-implicit spit operator (PISO) algorithm [13]. PISO algorithm applies mass conservation into pressure equation, thus when pressure equation converges, continuity error decreases. This method uses a predictor-corrector on solving pressure-velocity coupling, and utilizes a collocated grid method [14].

VOF Method

The Volume of fluid (VOF) method with bounded compression techniques is applied to control numerical diffusion and capture the two-phase interface efficiently. The VOF transport equation is described below:

$$\frac{\partial \alpha}{\partial t} + \nabla \cdot [(\mathbf{U} - \mathbf{U}_{g})\alpha] = 0 \tag{3}$$

Where α is volume of fraction, indicating the relative proportion of fluid in each cell and its value is always between zero and one:

$$\begin{cases} \alpha = 0 & \text{air} \\ \alpha = 1 & \text{water} \\ 0 < \alpha < 1 & \text{interface} \end{cases} \tag{4}$$

6DOF Motions and Patch forces

A fully 6DOF module with bodies is implemented. Two coordinate systems are used to solve 6DOF equation. We describe $(x_1, x_2) = (x, y, z, \varphi, \theta, \psi)$ as the translation and rotation angles of the ship, representing motions of surge, sway, heave, roll, pitch and yaw, respectively. $(v_1, v_2) = (u, v, w, p, q, r)$ are the velocities in the earth-fixed coordinate system, which can be transformed to the body-fixed coordinate system by equations given below:

$$v_1 = J_1^{-1} \cdot \dot{x}_1 \qquad v_2 = J_2^{-1} \cdot \dot{x}_2 \tag{5}$$

where J_1, J_2 are transformation matrices based on Euler angle. The forces and moments are projected into the earth-fixed system in following way:

$$F = (X, Y, Z) = J_1^{-1} \cdot F_e \qquad M = (K, M, N) = J_1^{-1} \cdot M_e \tag{6}$$

In order to compute the sloshing forces and moments, the single body is divided into several patches. In present study, the single body is divided into three patches: the hull of FLNG which can reveal external forces and moments, the left side of inner tank and the right side of inner tank. The forces are integrated on each patch separately, and accumulated as a whole to compute for next motion. The process is shown in Fig.1.

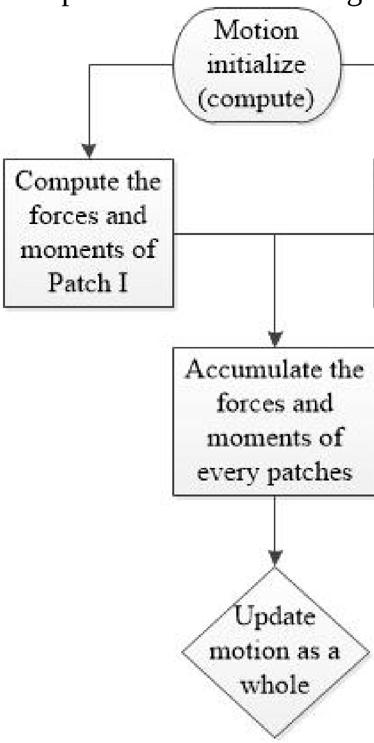

Figure 1. The algorithm for calculating the forces and moments of each patch

Wave Generation and Damping

The incoming regular wave is generated by imposing the boundary conditions of α and **U** at the inlet. The linear Stokes wave in deep water is applied for the wave generation.

$$\xi(x,t) = a\cos(kx - \omega_e t) \tag{7}$$

$$u(x,y,z,t) = a\omega e^{kz}\cos(kx - \omega_e t) \tag{8}$$

$$w(x,y,z,t) = a\omega e^{kz}\sin(kx - \omega_e t) \tag{9}$$

where ξ is the wave elevation; a is the wave amplitude; k is the wave number; U_0 is the ship velocity; ω is the natural frequency of wave; ω_e is the encounter frequency, in this condition, $\omega_e = \omega$.

Numerical Results

Geometry and mesh generation

The chosen model is simplified LNG FPSO [11]. The main particulars of ship-shaped FPSO vessel in both full scale and model scale are illustrated in Table 1.

Table 1. Main particulars of LNG FPSO.

Main particulars		Full Scale	Model
Scale factor	—	1	1/100
Length between perpendiculars	L_{PP} (m)	285	2.85
Maximum beam of waterline	B_{WL} (m)	63	0.63
Draft	T (m)	13	0.13
Displacement	Δ (m^3)	220017.6	220.0176
Natural period of roll	$T_{\emptyset}$ (s)	13	1.3
Vertical Center of Gravity (from keel)	KG (m)	16.5	0.165
Radius of gyration	K_{xx}	19.45	0.1945
	K_{yy}	71.25	0.7125

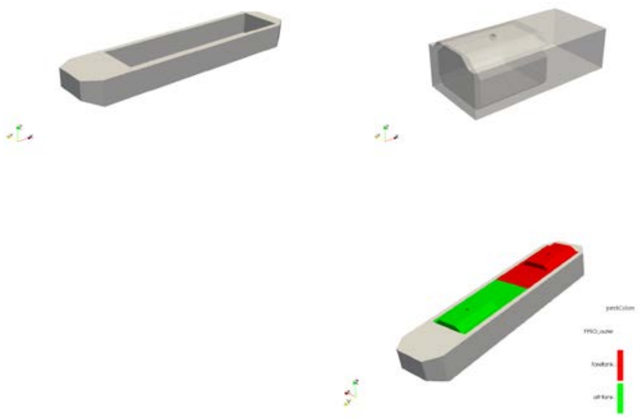

Figure 2. The geometry of each part from FPSO and inner tanks

The model scaled LNG FPSO and computational domain setup is shown in Fig.3. The filling condition is also included, shows that 82.6% filling ratio in fore tank, and 23.5% filling ratio in aft tank. The computational domain was set as $-1.0L_{pp}<x<2.0L_{pp}$, $-1.5L_{pp}<y<1.5L_{pp}$, $-1.0L_{pp}<z<1.0L_{pp}$. The sponge layer was included to avoid the wave reflection and keep mass conservation in computational domain. The FPSO was restrained to heave, roll and pitch motion.

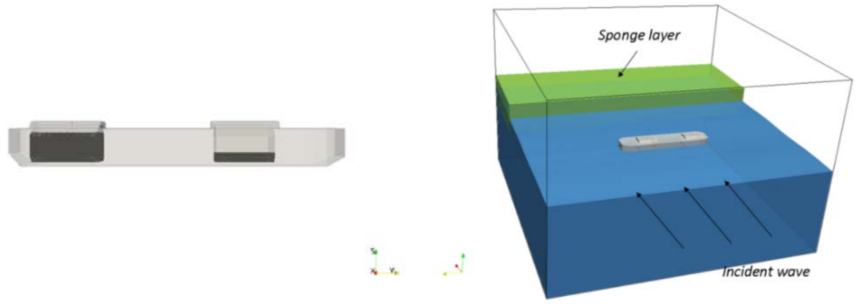

Figure 3. The geometry and computational domain setup

The meshes are generated by snappyHexMesh, an auto mesh generation utility provided by OpenFOAM. The total cell numbers are around 2.1M, and the LNG tanks require 0.5M cells. The mesh details are shown in Fig. 4. The right side of picture in Fig.4 shows two small tunnels connected the LNG tanks to the external region, which can keep the pressure inside the tanks same to the external region and simplify the computations. Meanwhile, the connection tunnel makes the computation fully coupled.

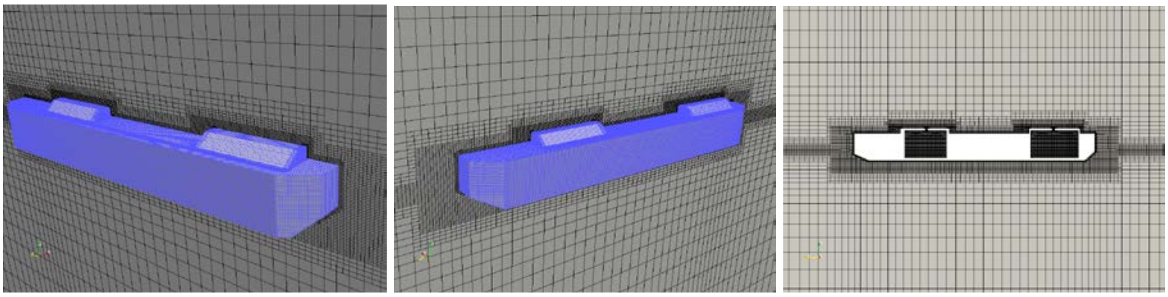

Figure 4. Demonstrations of meshes

Numerical verification

The roll motion response in frequency domain is shown in Fig.5. The normalized motion amplitude and natural frequency are considered to compare with experimental data. The normalized roll motion is given as: $\theta B/2A$, in which θ is maximum degree of roll motion, B is beam of ship and A is wave amplitude. The normalized natural frequency is given as: $\omega(L/g)^{1/2}$, in which ω is natural frequency of water, L represents length of ship.

In order to compare with the existing experimental data, the simulations are all under the same incident wave height, which is 0.025m. Two different incident wave frequencies are considered, and the normalized wave frequencies were chosen to be 2.5 and 3.5 separately. Fig.5 indicates the comparison of roll motion between present work and experiment. Besides, the results of other numerical results were also included. The potential theory [15] adopted in 20% filling conditions cannot simulate the 82.6% filling ratio, for the high filling condition reach the top corner of the LNG tank and the linear potential theory did not have the ability to simulate it. The results of circumstances were better than other simulation results when compared to the experimental data, showing an advantage in simulating the hybrid of high-filling condition and low-filling condition. Some of the results about 20% filling condition were from the work done before [10], and the case of normalized wave frequency equals to 3.5 was new added in this paper. The results of current study show well agreement with experimental results, which proves that our methods are reliable.

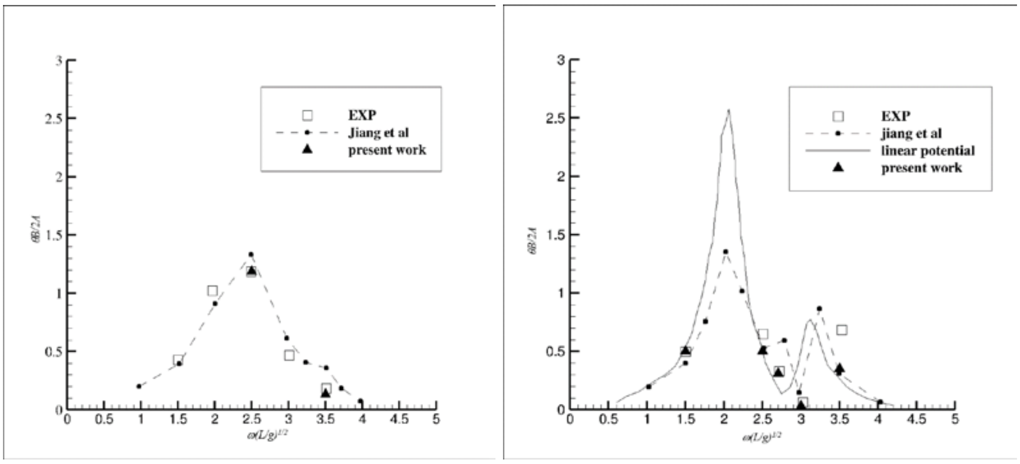

Figure 5. Comparison among current studies and experiments and other numerical methods.(left 82.6%-23.5%, right 20%-20%)

It can be observed that the 20% filling conditions had two peaks of roll motion response, while the 82.6%-23.5%filling condition only had one peak. To better understand the coupling effects between ship motion and sloshing tanks, and the coupling effects of two sloshing tanks as well, the inner sloshing moments and external exciting moments were discussed.

Sloshing moment and external exciting moment

The sloshing moments of 82.6%-23.5% filling condition were shown in Fig.6. The sloshing moments of fore tank and aft tank were compared in normalized moment. It can be seen that under these two wave frequencies, the external wave force produce larger moment on the low filling ratio tank. Under different wave frequencies, the time history of moment from each tank shows different phenomenon. In the normalized wave frequency of 2.5, the moment curve of fore tank (82.6% filling ratio) and the aft tank (23.5%) did not show phase difference. However, in the normalized wave frequency equals to 3.5, the time history of moment in each tank shows the phase difference, almost near 180 degree. The phase difference means under this wave frequency, the sloshing moments in aft tank and fore tank influence each other, and reduce the total sloshing moment which was acted on FPSO.

Considering the external exciting moment, shown in Fig.7, it can be observed that the time history of fore tank moment have phase difference with external exciting moments under both wave conditions. That’s the reason why the sloshing fluid can reduce the ship motion. Besides, the number of sloshing moment and exciting moment under the case of normalized wave frequency equals to 3.5 is much smaller than that in the case of 2.5, therefore the roll motion of 3.5 case was smaller than that of 2.5 case.

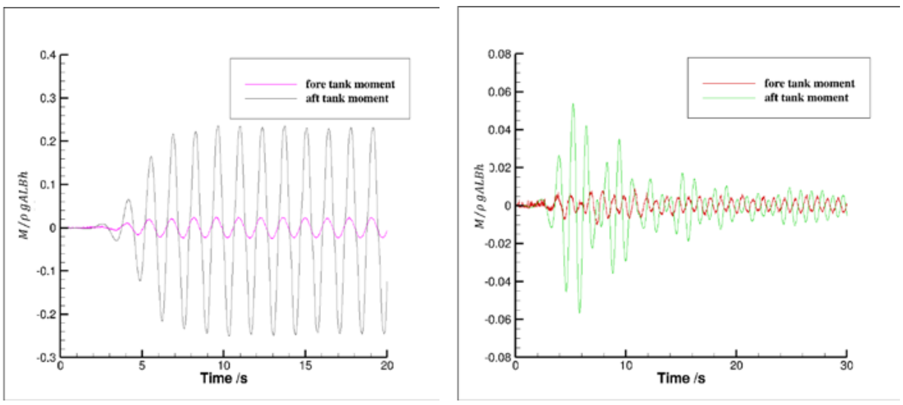

Figure 6. Time history of inner sloshing moment in aft and fore tank in different wave frequencies. (filling ratio 82.6%-23.5%, from left to right: normalized wave frequency 2.5, 3.5.)

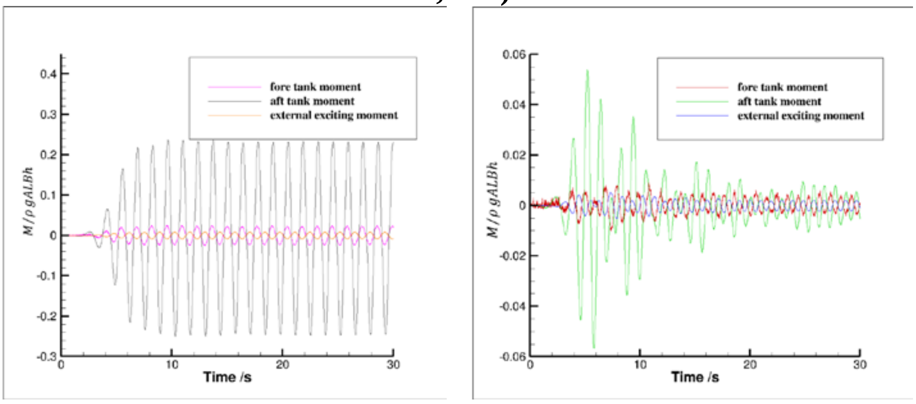

Figure 7. Time history of inner sloshing moment in aft and fore tank and external exciting moment in different wave frequencies. (filling ratio 82.6%-23.5%, from left to right: normalized wave frequency 2.5, 3.5.)

Fig.8 illustrated the sloshing moment of 20%-20% filling condition. For the filling ratios were the same in fore and aft tanks, the sloshing moments were also the same. Fig.9.included the external exciting moments. It can be observed that in the case of 2.5, the external exciting moments showed phase difference with the sloshing moment. The degree of phase difference were almost 180 degree. The external exciting moment excited the sloshing moments, while the sloshing moment reduced the external exciting moment in return. However, the case that normalized wave frequency equals to 3.5 were totally different. The phase of sloshing moment and exiting moment were the same. Although the external exiting moment in case of 3.5 was smaller than that in case of 2.5, the induced sloshing moment increase the total moment acted on ship. Therefore, the value of roll ship motion didn't show difference between these two cases.

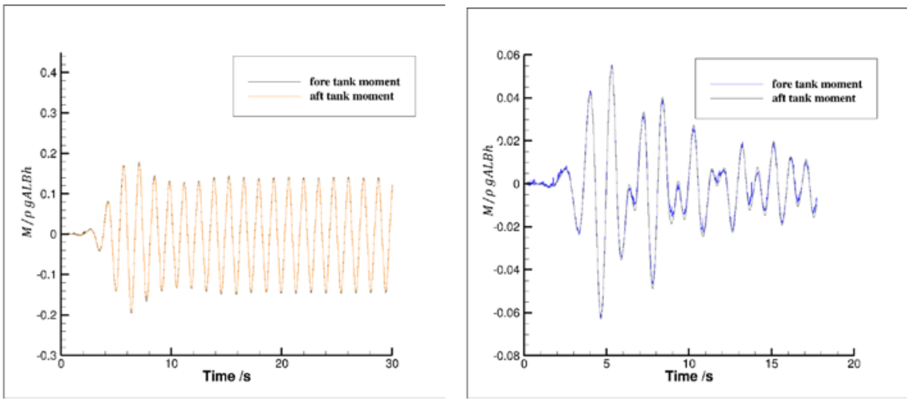

Figure 8. Time history of inner sloshing moment in aft and fore tank and external exciting moment in different wave frequencies. (filling ratio 20%-20%, from left to right: normalized wave frequency 2.5, 3.5.)

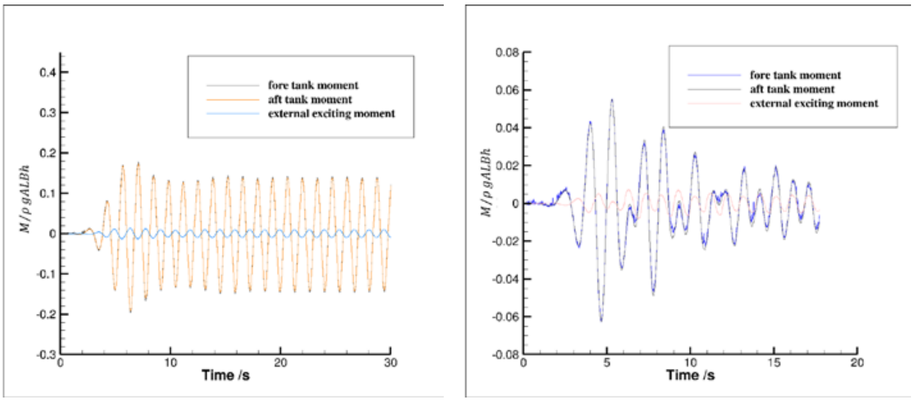

Figure 9. Time history of inner sloshing moment in aft and fore tank and external exciting moment in different wave frequencies. (filling ratio 20%-20%, from left to right: normalized wave frequency 2.5, 3.5.)

Sloshing flow

To observe the coupling effects, the internal tank flow were included. Fig.10 shows three snapshots of sloshing flow in fore tank and aft tank. The images of fore tank and aft tank were all in the same time. To better observe the detail of sloshing flow, the snapshots of fore tank had mirror reversal. Thus the phase of sloshing flow in fore tank and aft tank were the same, just accord with the sloshing moment shown before.

The sloshing flow in fore tank is almost linear, for the filling ratio is high. While in aft tank appeared a wave crest among the sloshing flow. This peak moved along with ship, probably induced by ship motion. To better observe the sloshing flow, we simulated a large wave height case, shown in Fig.11, where the wave height equals to 0.1m. It can be seen that the sloshing flow in high filling condition tank was still linear, and it had a phase difference with external flow. Due to the low-filling condition, the sloshing flow in aft tank showed a great nonlinearity. The inner fluid broke on the bulkhead, and formed a propulsion wave that moved with ship motion. And then the propulsion wave reached the other bulkhead, and broke on the bulkhead. In order to observe the sloshing flow in aft tank, the velocity vector of the wave crest was included and shown in Fig.12. The velocity distribution along the tank length was not the same because of the pitch motion. The direction of velocity in wave crest changed when the propulsion wave on its way to the bulkhead, thus wave rolled over during the propulsion. This kind of sloshing flow showed a phenomenon like that of shallow water wave.

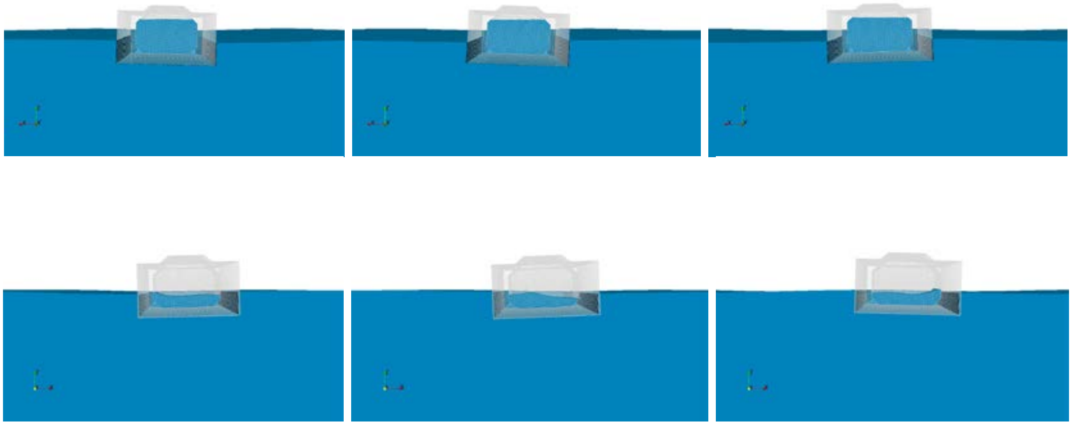

Figure 10. Snapshots of inner tank flow and outer flow (above were fore tank filling 82.6%, bottom were aft tank filling 23.5%; normalized wave frequency is 2.5)

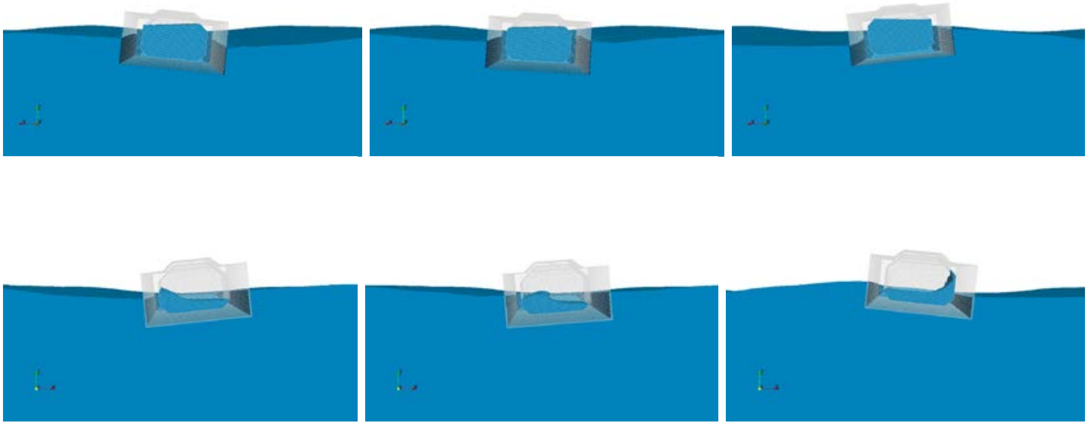

Figure 11. Snapshots of inner tank flow and outer flow in wave height equals 0.1m. (above were fore tank filling 82.6%, bottom were aft tank filling 23.5%; normalized wave frequency is 2.5)

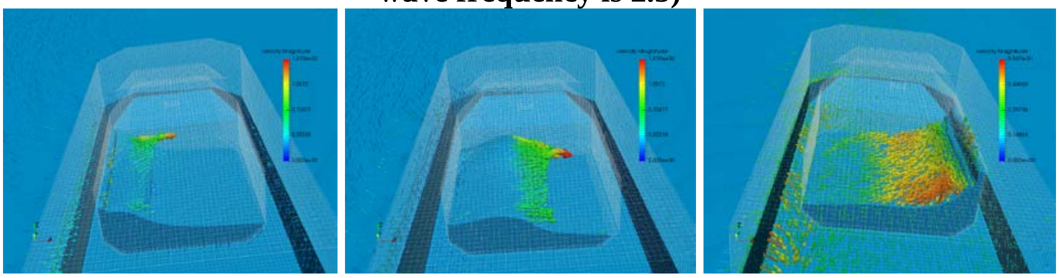

Figure 12. Velocity vector of inner tank flow and outer flow in wave height equals 0.1m. (above were fore tank filling 82.6%, bottom were aft tank filling 23.5%; normalized wave frequency is 2.5)

Conclusions

In this paper, the coupling effects were discussed using our in house solver naoe-FOAM-SJTU. The LNG FPSO was equipped with two different filling ratio tanks, and both the ship motion and sloshing moments were considered. The roll motion in different wave frequencies of FPSO were compared with experimental results, and showed well agreement, which revealed our solver had the advantages to solve both the high filling condition and low filling condition. Through observing the results, we found that the roll motion of 82.6%-23.5% filling condition reduced at the case that normalized wave frequency equals to 3.5, while that of 20%-20% was almost the same. In order to figure it out, the study of sloshing moments was carried out.

Our in house CFD solver naoe-FOAM-SJTU has added new functions to solve the problem. The model was departed into inner and outer parts to obtain the sloshing moments and external exciting moments. The results were analyzed to figure out how the sloshing moments influence the ship motion. The sloshing moments in tanks have a phase difference with external exciting moments when the normalized wave frequency equals to 2.5, thus the existence of sloshing tank would reduce the ship motion. When the normalized wave frequency equals to 3.5, In the case of 82.6%-23.5%, not only the sloshing moment in fore tank and aft tank showed phase difference, but external exciting moments showed the phase difference as well; whereas in the case of 20%-20%, both the sloshing moments in fore tank and aft tank and external exciting moments were in the same phase, therefore the ship roll motion didn't reduce as that in case of 82.6%-23.5%.

At last, the sloshing flow and velocity were included to observe the details of sloshing flow. For the high filling condition, the sloshing flow is almost linear even under large wave height. However, the low filling condition shows the nonlinearity both under small wave height and large wave height. The break and roll over were observed under large wave height condition.

In the future, the wave height in the tank would be observed to deeper understand the relationship between external wave excitation and internal flow. Different wave direction would be considered.

Acknowledgements

This work is supported by the National Natural Science Foundation of China (51379125, 51490675, 11432009, 51579145), Chang Jiang Scholars Program (T2014099), Shanghai Excellent Academic Leaders Program (17XD1402300), Program for Professor of Special Appointment (Eastern Scholar) at Shanghai Institutions of Higher Learning (2013022), Innovative Special Project of Numerical Tank of Ministry of Industry and Information Technology of China (2016-23/09) and Lloyd's Register Foundation for doctoral student, to which the authors are most grateful.

References

[1] Rognebakke, O. F., Faltinsen, O. M. (2003) Coupling of sloshing and ship motions, *Journal of Ship Research* **47**, 208-221.
[2] Newman, J. N. (2005) Wave effects on vessels with internal tanks. *In: Proceedings of the 20th Workshop on Water and Floating Bodies*. Sptisbergen, Massachusetts.
[3] Seo, M. G., Kim, Y., and Park, D. M. (2017). Effect of internal sloshing on added resistance of ship. *Journal of Hydrodynamics*, Ser. B, **29**, 13-26.
[4] Lee, S. J., Kim, M. H., Lee, D. H. and Shin, Y. S. (2007) The effects of tank sloshing on LNG vessel response. *In: Proceedings. of 26th International Conference on Offshore Mechanics and Arctic Engineering*, San Diego, California, OMAE 2007-29665.
[5] Li, Y. L., Zhu, R. C., Miao, G. P. and Fan, J. (2012) Simulation of tank sloshing based on OpenFOAM and coupling with ship motions in time domain. *Journal of Hydrodynamics*, Ser. B, **24**, 450-457.
[6] Kim, J. W., Kim, K. (2007) Response-based evaluation of design Sloshing loads for membrane-type LNG carriers. *In: Proceedings of 26th International Conference on Offshore Mechanics and Arctic Engineering*. San Diego, USA, OMAE2007-29746.
[7] Jiang, S. C., Teng, B., Bai W., Guo, Y. (2015) Numerical simulation of coupling effect between ship motion and liquid sloshing under wave action. *Ocean Engineering*, **108**, 140-154
[8] Li, X., Zhang, T., Zhang, Y. O., and Wang, Y. X. (2014, April). Numerical analysis of ship motion coupled with tank sloshing. *In OCEANS 2014-TAIPEI* IEEE, 1-10.
[9] Shen, Z. R. and Wan, D. C. (2012) Numerical Simulations of Large-Amplitude Motions of KVLCC2 with Tank Liquid Sloshing in Waves. *In Proceedings 2nd Int Conf Violent Flows*. Ecole Centrale Nantes, Nantes, France.
[10] Zhuang, Y. and Wan, D. C. (2016) Numerical Study on Coupling Effects of FPSO Ship Motion and LNG Tank Sloshing in Low-Filling Conditions. *Applied Mathematics & Mechanics*, **37**, 1378-1393.
[11] Nam, B. W, Kim, Y., Kim, D. W., Kim, Y. S. Experimental and Numerical Studies on Ship Motion Responses Coupled with Sloshing in Waves. *Journal of Ship Research*, 2009, **53**, 68-82.
[12] Issa, R. I. (1986). Solution of the implicitly discretized fluid flow equations by operator-splitting. *Journal of computational physics*, **62**, 40-65.
[13] Rhie, C. M. and Chow, W. L. (1983). Numerical study of the turbulent flow past an airfoil with trailing edge separation. *AIAA journal*, **21**, 1525-1532.
[14] Dhakal, T. P. and Walters, D. K. (2009, January). Curvature and rotation sensitive variants of the K-Omega SST turbulence model, *In ASME 2009 Fluids Engineering Division Summer Meeting*. American Society of Mechanical Engineers. 2221-2229.

[15] Guo, Y., Kim, Y., Kim, T. Y. (2011) A numerical study on coupling between ship motions and sloshing in frequency and time domain. *Proceedings of the 21th International Offshore and Polar Engineering Conference*, Maui, Hawaii, USA, 158-164.